Increasing Al-pair abundance in SSZ-13 zeolite via zeolite synthesis in the presence of alkaline earth metal hydroxide produces hydrothermally stable Cobalt and Pd-SSZ-13 materials for pollutant abatement applications

Konstantin Khivantsev[1*]†, Miroslaw A. Derewinski[1,2*]†, Nicholas R. Jaegers[1], Daria Boglaienko[1], Xavier Isidro Pereira Hernandez[1], Carolyn Pearce[1], Yong Wang[1,3] and Janos Szanyi[1*]†

[1]Pacific Northwest National Laboratory Richland, WA 99352 USA

[2] J. Haber Institute of Catalysis and Surface Chemistry, Polish Academy of Sciences, Krakow 30-239, Poland

[3] The Gene and Linda Voiland School of Chemical Engineering and Bioengineering, Washington State University

Pullman, WA 99164-6515

We dedicate this study to Mirek Derewinski on occasion of his 70th birthday and remarkable contributions to the field of zeolite synthesis, chemistry, and reactivity!

*corresponding authors: MAD, KK, JSz

†these authors contributed equally: KK , MAD, JSz

We show that replacing alkaline (NaOH) for alkaline-earth metal ($Sr(OH)_2$ as an example) in the synthesis of SSZ-13 zeolite with Si/Al~10 produces SSZ-13 zeolite material with novel, advantageous properties. Its NH_4-form ion-exchanges higher amount of Co(II) ions than the conventional one: this is the consequence of increased number of Al pairs in the structure induced by the +2 charge of Sr(II) cations in the synthesis gel that force two charge-compensating AlO_4^- motives to be closer together. We characterize the +2 state of Co(II) ions in these materials with infra-red spectroscopy and XANES measurements. They can be used for NOx pollutant adsorption from ambient air: the ones derived from SSZ-13 with higher Al pair content contain more cobalt(II) and thus, perform better as ambient-air NOx adsorbers before reaching full saturation capacity. Notably, Co(II)/SSZ-13 material with increased number of Al pairs is significantly more hydrothermally stable than its NaOH-derived analogue. Loading 1.7 wt% Pd into Co-SSZ-13 synthesized in the presence of Sr(II) produces an active passive NOx adsorber (PNA) material that can be used for NOx adsorption from simulated diesel engine exhaust. The critical issue for these applications is hydrothermal stability of Pd-zeolites. Pd/SSZ-13 synthesized in NaOH media loses most of its PNA capacity after ~800 ºC hydrothermal aging in the flow of air and steam (10 hours in 10% H_2O/air flow). The 1.7 wt% Pd/Co/SSZ-13 material with Si/Al ~10 does not lose its PNA capacity after extremely harsh aging at 850 and 900 ºC (10 hours in 10% H_2O/Air flow) and loses only ~55% capacity after hydrothermal aging at 930 ºC. It shows considerably enhanced stability compared with previous record for Pd/FER, Pd/SSZ-39 and Pd/BEA materials that could survive hydrothermal aging no higher than 820 ºC. We herein reveal a new, simple, and scalable strategy for making remarkably (hydro)thermally stable metal-zeolite materials/catalysts with a number of useful applications.

Within the last decade, Metal/zeolites system became the front-liners of environmental catalysis [1,2]. These materials/catalysts have allowed to tackle the most challenging environmental problems caused by pollutant emitted by the vehicles [1-7]. More specifically, nitric oxide is a free-radical harmful pollutant, even more dangerous than carbon monoxide (CO). Nearly 55% of the global NOx emissions come from vehicles [1,8-10]. Cu/zeolite materials have been successfully commercialized to scrub NOx and turn it into environmentally clean dinitrogen in diesel vehicles [1-7]. Sacrificial ammonia reductant is used, and this catalytic reaction is effective at temperatures starting 180 ºC with state-of-the-art catalyst formulations. Significant advances have been achieved in understanding the fundamental nature of catalytic SCR reaction on Cu/SSZ-13 and Cu/BEA zeolitic systems [1-7,11-18]. Although Cu/SSZ-13 catalysts show excellent activity above 200 ºC, no catalysts were shown to be active at lower temperatures. Only recently have we discovered that NO^+ ions in zeolites (formed via $NO+O_2$ reaction) catalyze direct reduction of NO^+ with NH_3 to nitrogen at room temperature and below [18]. The process can be run catalytically when some NH_3 can desorb from zeolite [18]. However, higher temperatures require Cu(II) ions presence due to, in part, ability to form Cu(I)---NO^+ site by direct Cu(II) reduction with free-radical NO. Emissions

during vehicle cold start, however, remain a challenge. To circumvent this challenge, Pd/zeolite materials (passive NOx adsorbers) have been introduced industrially that adsorb NO strongly as Pd(II)-NO, Pd(I)-NO, Pd(II)(OH)(NO) and Pd(II)(NO)(CO) complexes (depending on Pd speciation in zeolites) at low temperatures (80-130 ºC) during cold start and then release them at higher temperatures (>170-180 ºC) when downstream SCR catalysts become very active [19-35]. The main challenge for application of Metal/zeolite materials for industrial vehicle use has always been their hydrothermal stability. They may be exposed in vehicles to harsh steam treatment (during diesel particular filter regeneration, for example) [19-33]. In general, it is desirable to develop materials that can survive hydrothermal aging at temperatures as harsh as 800 ºC and higher. For passive NOx adsorbers, the highest known survival temperatures are 750-820 ºC [19-33]. For example, we have been able to engineer Pd/BEA crystals that can survive 750 ºC hydrothermal treatment without any deterioration [21]. For SSZ-13 materials prepared via regular method (in the presence of NaOH and N(adamantyl) structure-directing agents) 750 ºC hydrothermal aging (HTA) already leads to erosion of some Pd(II) ions and their transformation into nanoparticles on the external zeolite surface, likely through Pd aluminate and $Pd_x(OH)_y$ species formation in the presence of water (with simultaneous framework dealumination) [25-27, 34, 35]. Therefore, there is an urgent need to develop hydrothermally stable SSZ-13 materials. It is important to note that the Si/Al ratio of zeolite plays an important part in stability: the higher the Si/Al ratio, the more hydrophobic the inner pore of zeolite is (considering no significant amount of other defects are present), and the more resistant to steam HTA treatment it is [21,27]. However, as we convincingly showed recently, with increase of Si/Al ration from 6 to 10-12 to 20-30, hydrophobicity of the pores leads to exclusion of atomically dispersed M(II) species and formation of MOx nanoparticles on the external surface (due to hydrophobicity of the pore and the inability of the aqua hydroxo complexes of metal to get “inside”) [20,22,25]. Furthermore, Pd distribution changes with increase of Si/Al ratio: for SSZ-13 with Si/Al ratio 6, Pd was almost completely atomically dispersed and present exclusively as Pd(II) ions held by proximal AlO_4^- pairs [20,22]. For sample with Si/Al ratio 10-12, around ~80-90% Pd was atomically dispersed and present as a mixture of Pd(II) and Pd(II)-OH species [20,22]. For sample with higher Si/Al ratio much less (<30%) of Pd was atomically dispersed and present exclusively as Pd(II)-OH species [20,22]. Pd(II) ions are more active and stable towards PNA. Thus, we chose to focus on the zeolite with Si/Al ~10 (providing higher hydrothermal stability than Si/Al~6) that can still accommodate most of Pd as atomically dispersed species. Furthermore, for the sample with Si/Al ~5-6 most of Al would be present as proximal pairs, most likely, irrespective of synthesis conditions due to significant abundance of Al. However, for higher Si/Al ratios statistically speaking less Al sites will be proximal and thus it would be harder to create the desired M(II)

sites. We hypothesized that we could create more Al paired sites by introducing alkaline earth metals (such as $Sr(OH)_2$ or $Ba(OH)_2$) in the synthesis gel instead of typically used NaOH. We focused on Sr specifically rather than Ba, because Ba is extremely toxic (however, we believe barium hydroxide would probably have similar effect as strontium hydroxide). $Sr(OH)_2$ has some issues with solubility at room temperature (it takes some stirring to dissolve it) but at higher temperature of the typical hydrothermal autoclave synthesis it has excellent solubility. Sr(II) has a charge of +2, and it would require two proximal AlO_4^- units to produce the resulting Sr(II)-form zeolite compared with 1 AlO_4^- unit required to stabilize Na-form zeolite [3].

After synthesis, the resulting Sr/SSZ-13 and Na/SSZ-13 were centrifuged and washed with DI water multiple times. NH_4-ion exchange was performed multiple times with ammonium nitrate to produce NH_4-forms of zeolite.

It is universally accepted that the measure of amount of Al pairs in zeolitic materials can be determined by Co(II) ion exchange capacity [37-41]. Co(II) ions are generally assumed to exist almost exclusively as Co(II)/2Al species in zeolites. We exchanged both NH_4-SSZ-13 samples with Co(II) ions under identical conditions and calcined in the air flow at 650 ºC. The resulting blue-powders with isolated Co(II) ions in distorted tetrahedral environment [42] on air slowly (~5-7 days) regain the pink color due to moisture adsorption and coordination of moisture to tetrahedral Co to form square-pyramidal and octahedral Co aqua complexes (Fig. S1) [42]. XANES characterization for both samples shows that Co is present in +2 oxidation state. XANES for the Co/ sample prepared from SSZ-13(Sr) showed better signal intensity than for the one prepared from SSZ-13(Na), already suggesting to us that Cobalt is present in higher amounts (Fig. S2) [samples were prepared with approx. similar masses of sample and similar pressed tablets]. With infra-red spectroscopy we looked at NO adsorption on Co/SSZ-13 material (Fig. 1A). NO adsorption produces two NO stretches that grow in concert upon NO titration. They belong to $Co(II)(NO)_2$ complex [42-50] with symmetric NO stretch at 1900 cm^{-1} and asymmetric NO stretch at 1816 cm^{-1}. This is typical for atomically-dispersed Co(II) ions in zeolite [42-50]. Co ions exist in extra-framework positions and not in silanol nests/silica matrix: the latter vibrate at slightly lower frequencies [42-50]. Importantly, 1 cobalt ion can adsorb up to 2 NO molecules. $Co(NO)_2$ complexes survive under vacuum at elevated temperature (Fig. 1b). This suggested to us Co/SSZ-13 materials would be useful for NO adsorption from ambient air. NO is a nuisance pollutant and Co-containing systems have previously shown promise for NO adsorption from ambient air. For these materials, it would be important to maximize the number of Co(II) ions per SSZ-13 mass: the amount of adsorbed cobalt correlates linearly with the number of Al pairs in SSZ-13

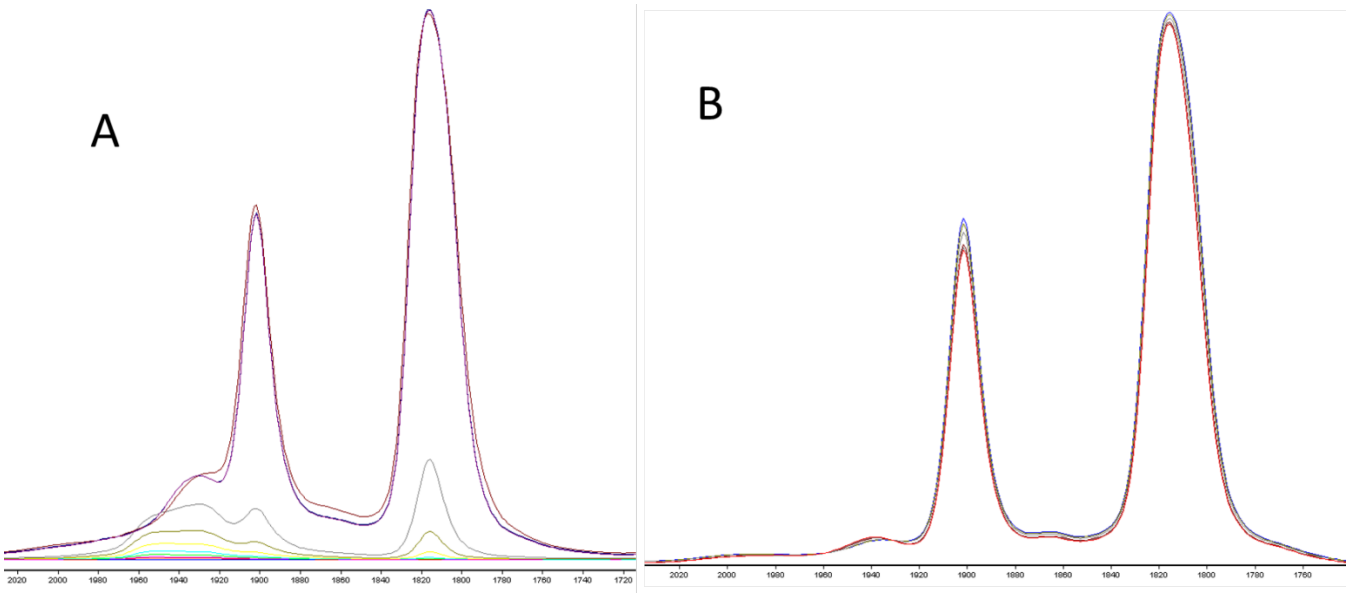

Figure 1. A. In-situ FTIR during NO adsorption (~2 Torr) at room temperature on activated Co-SSZ-13. NO bands at 1900 and 1816 cm^{-1} belong to $Co(II)(NO)_2$ complex. Minor band at 1930 cm^{-1} belongs to NO adsorbed on Co(III) ions of polynuclear cobalt oxide clusters. B. NO desorption from $Co(II)(NO)_2$ under vacuum (10^{-6} Torr) at 80 ºC. $Co(II)(NO)_2$ complex shows resistance to decomposition.

material. Indeed, both Co/SSZ-13(Na) and Co-SSZ-13(Sr) are active for NO adsorption (Fig. 2). However, the material derived from Sr/SSZ-13 stores at least 55% more NO compared with Co-SSZ-13(Na).

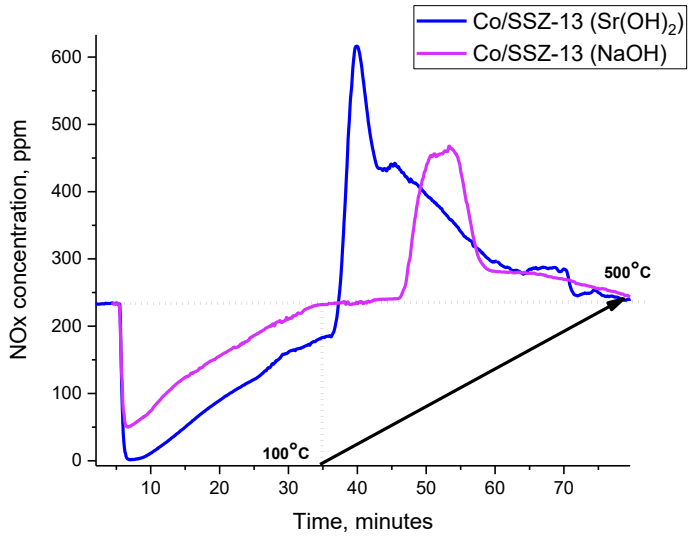

Figure 2. NOx adsorption on Co-SSZ-13 samples derived from NaOH and Sr(OH)2 synthetic routes at 100 °C for 30 min (after 5 min bypass) followed with TPD (10 °C/min). The feed gas mixture contains ~220 ppm of NOx, 14% O_2 and ~300 ppm H_2O. Sample mass 120 mg. Total flow rate ~ 300 sscm/min.

It is more advantageous for NO adsorption applications and it lasts long as a NO adsorber at ambient temperature from ambient air (Fig. 3).

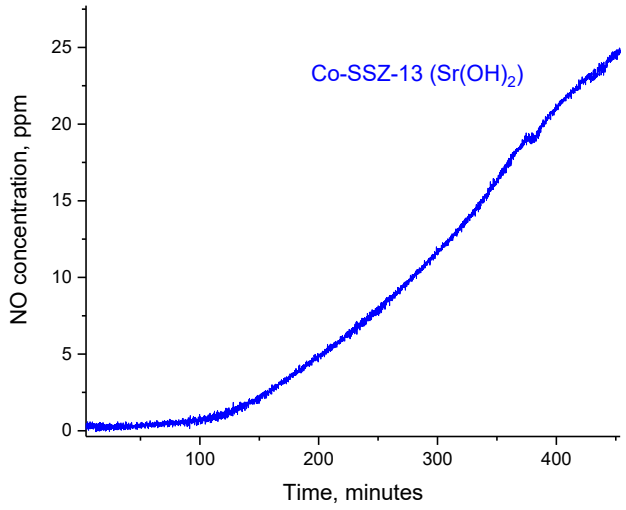

Figure 3. NOx adsorption on Co-SSZ-13 samples derived from $Sr(OH)_2$ synthetic route at 23 °C while flowing gas mixture containing ~27 ppm of NO, 20% O_2 and ~300 ppm H_2O (adoption of NO from ambient air allows to keep NO level below 2 ppm for ~160 minutes). Sample mass 120 mg. Total flow rate 300 sscm/min.

The higher number of Al pairs is the direct consequence of $Sr(OH)_2$ use during SSZ-13 synthesis. We also tested this material as a PNA material for vehicle exhaust. Despite its ability to absorb NOx during vehicle cold start, Co/SSZ-13 is not viable for NO_x adsorber applications because it releases NO_x too early (Fig.4).

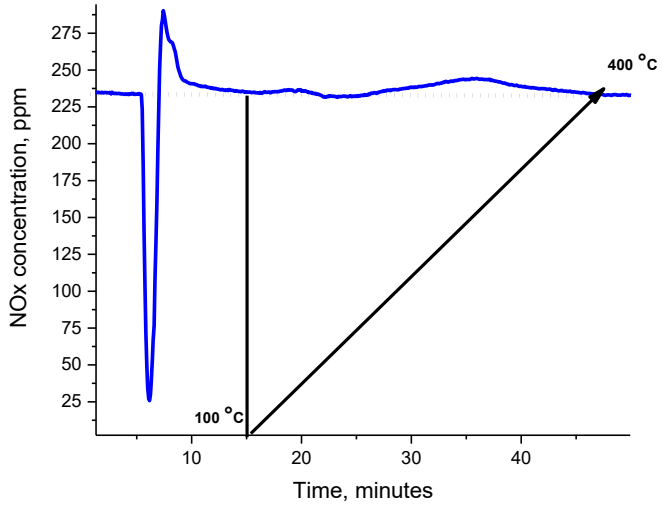

Figure 4. NOx adsorption on Co-SSZ-13 samples derived from Sr(OH)2 synthetic route at 100 °C for 30 min (after 5 min bypass) followed with TPD (10 °C/min). The feed gas mixture contains ~220 ppm of NOx, 200 ppm CO, 14% O_2 and ~3% H_2O. Sample mass 120 mg. Total flow rate ~ 300 sscm/min.

However, it is important to note that presence of Co ions is not detrimental for NO storage (unlike for Na-containing materials, for example as outlined in our previous study [25]). The presence of higher fraction of paired Al sites in Co/SSZ-13(Sr) compared with Co-SSZ-13(Na) prompted us to investigate whether this sample possesses higher hydrothermal stability. Remarkably, even though HT aging Co-SSZ-13(Na) at 850 ºC almost completely destroys its NO storage capacity, hydrothermal aging of Co-SSZ-13(Sr) at at 850 ºC and then further 900 ºC preserves its NO storage capacity/uptake (Fig. 5).

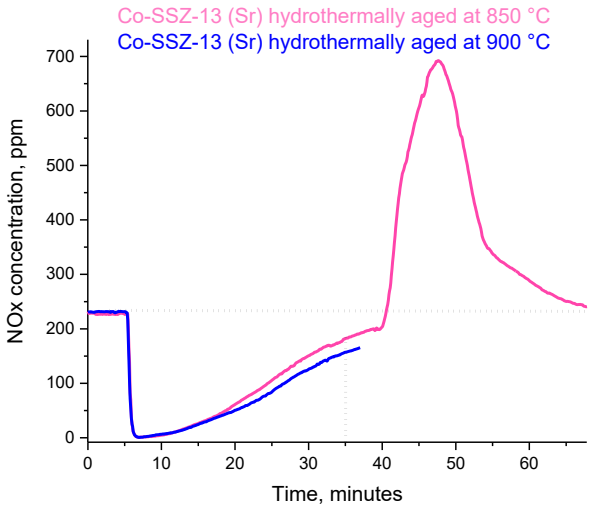

Figure 5. NOx adsorption on Co-SSZ-13 sample derived from $Sr(OH)_2$ synthetic route at 100 °C for 30 min (after 5 min bypass) followed with TPD (10 °C/min). The feed gas mixture contains ~220 ppm of NOx, 14% O_2 and ~300 ppm H_2O. Sample mass 120 mg. Total flow rate ~ 300 sscm/min. The sample was first hydrothermally aged at 850 ºC and tested for PNA. Then it was further hydrothermally aged at 900 ºC and PNA adsorption capacity was recorded at 100 ºC for 30 minutes (after 5 minute bypass).

It means, that hydrothermal aging of this material at 900 ºC does not lead to Cobalt(II) ion removal from the framework or collapse of SSZ-13 zeolitic structure. This, to the best of our knowledge, is the first demonstration of metal-promoted SSZ-13 hydrothermal stability at temperatures as high as 900 ºC. This corroborates our intuitive suggestion that distribution of Al sites within zeolite framework is a key factor in zeolitic hydrothermal stability: the material with higher number of Al pairs (synthesized in the presence of alkaline earth metal hydroxide in the synthesis gel) shows much higher hydrothermal stability than its SSZ-13(Na) analogue. This remarkable property of Co/SSZ-13(Sr) material, thus, prompted us to load 1.7 wt% Pd in its micropores and study its PNA properties and hydrothermal stability of the resulting Pd-containing SSZ-13 composite [19-35]. Indeed, the sample shows excellent PNA performance after loading Pd in it (Fig. 6).

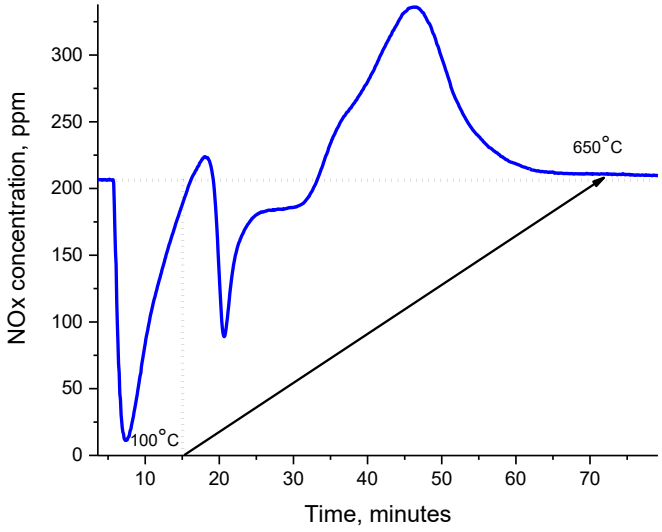

Figure 6. NOx adsorption on "fresh" 1.7 wt% Pd/Co-SSZ-13 sample derived from $Sr(OH)_2$ synthetic route at 100 °C for 30 min (after 5 min bypass) followed with TPD (10 °C/min). The feed gas mixture contains ~220 ppm of NOx, ~250 ppm CO, 14% O_2 and ~3% H_2O. Sample mass 120 mg. Total flow rate ~ 300 sscm/min.

The second NOx adsorption peak occurs during PNA on fresh Pd-Co-SSZ-13(Sr) sample at higher temperatures (that adsorption peak is absent for just Pd-SSZ-13 materials [20-23,25,27,28]). We thus attribute it to the presence of Co in the "fresh" sample. Previously, the best known Pd-zeolitic PNA materials could survive prolonged hydrothermal aging of 800-820 ºC. However, at higher temperatures they lost most of their performance (see, for example, our Pd-SSZ-39 and Pd/FER studies [27,33]). We first hydrothermally aged novel 1.7wt% Pd-Co-SSZ-13 material at 850 ºC for 10 hours in air/steam flow. Surprisingly, the low-temperature NOx adsorption band associated with Pd was fully preserved, and the sample was active as a PNA material (Fig. 7). Encouraged by this unprecedented result (no SSZ-13 material have been previously demonstrated to have such high hydrothermal stability), we further aged this material (after it was already aged at 850 ºC) for the same duration in air/steam flow at 900 ºC. To our delight, its PNA performance did not deteriorate (Fig. 7).

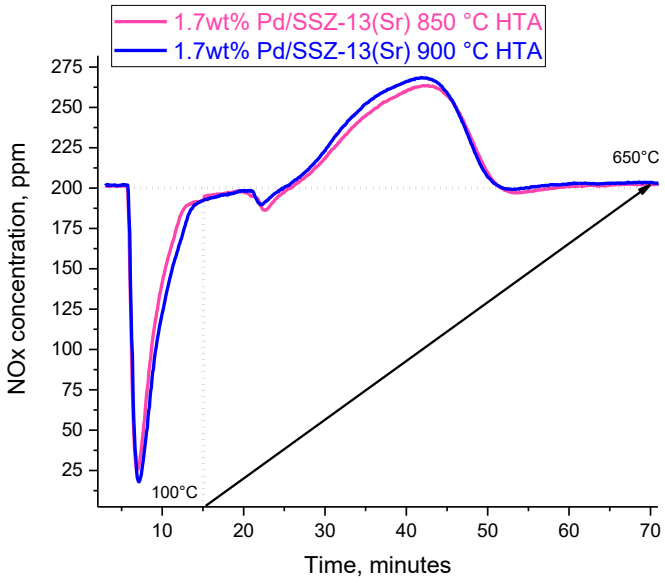

Figure 7. NOx adsorption on 850 and 900 ºC hydrothermally aged 1.7 wt% Pd/Co-SSZ-13 sample derived from $Sr(OH)_2$ synthetic route at 100 °C for 30 min (after 5 min bypass) followed with TPD (10 °C/min). The feed gas mixture contains ~220 ppm of NOx, ~250 ppm CO, 14% O_2 and ~3% H_2O. Sample mass 120 mg. Total flow rate ~ 300 sscm/min.

This is the most hydrothermally stable known PNA material ever reported. When we further hydrothermally aged this material (after it was aged at first at 850 ºC and then at 900 ºC) at 930 ºC for 10 hours in air/steam flow, 55% of PNA capacity was lost – still, some substantial PNA capacity was preserved and even such extremely harsh hydrothermal treatment did not lead to full collapse of the zeolitic material (Fig. 8).

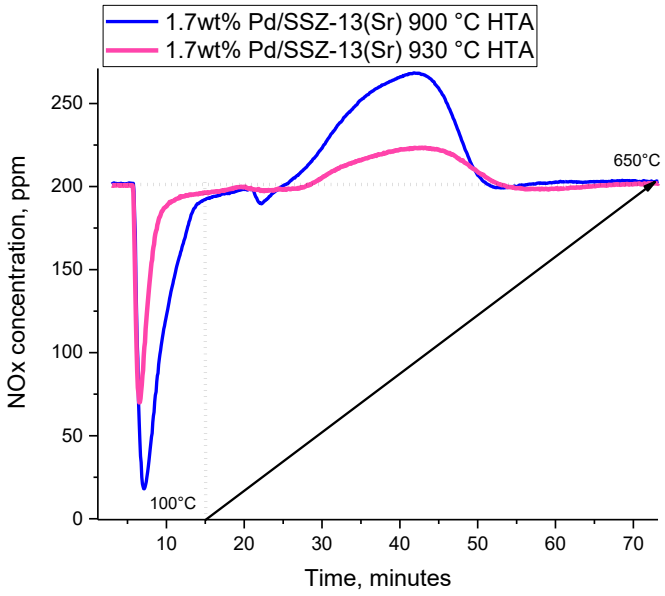

Figure 8. NOx adsorption on 900 and 930 ºC hydrothermally aged 1.7 wt% Pd/Co-SSZ-13 sample derived from $Sr(OH)_2$ synthetic route at 100 °C for 30 min (after 5 min bypass) followed with TPD (10 °C/min). The feed gas mixture contains ~220 ppm of NOx, ~250 ppm CO, 14% O_2 and ~3% H_2O. Sample mass 120 mg. Total flow rate ~ 300 sscm/min.

In summary, we report a simple and scalable method of increasing Al pairs distribution in siliceous SSZ-13 (Si/Al ratio at least 10). We show that this distribution is key in exchanging higher amounts of divalent metal cations (Co(II) and Pd(II), for example) atomically dispersed in the SSZ-13 micropores. The resulting materials have higher adsorption capacity for NO under different conditions. Furthermore, we show remarkable hydrothermal stability of the resulting metal zeolite materials that survive extraordinarily harsh hydrothermal aging conditions (encountered in vehicle exhaust under certain circumstances) at 900 ºC and that do not lose full NOx adsorption capacity at even higher temperatures (930 ºC). Our study opens up a pathway to prepare new zeolite and divalent metal-zeolite composites/catalysts with (hydro)thermal robustness not available before.

References

(1) Beale, A. M.; Gao, F.; Lezcano-Gonzalez, I.; Peden, C. H. F.; Szanyi, J. Chem. Soc. Rev. 2015, 44, 7371–7405.

(2) Liu, L., Corma, A. Nat Rev Mater (2020). https://doi.org/10.1038/s41578-020-00250-3
(3) Zones, S.I. US Pat 4 544 538, 1985.
(4) J.-H. Kwak, R. G. Tonkyn, D. H. Kim, J. Szanyi, C. H. Peden, J. Catal., 2010, 275, 187-190.
(5) I. Bull, A. Moini, G. Koermer, J. Patchett, W. Jaglowski, S. Roth, US Patent US20070134146A1, 2010.
(6) DW Fickel, RF Lobo, J. Phys. Chem. C 2010, 114 (3), 1633-1640.
(7) J.H. Kwak, D. Tran, S.D. Burton, J. Szanyi, J.H. Lee, C.H.F. Peden J. Catal., 287 (2012), p. 203.
(8) Royal College of Paediatrics and Child Health . Every breath we take—the lifelong impact of air pollution. London: Royal College of Paediatrics and Child Health, 2016.
(9) Sachtler W.M.H. (2002) Catalysis from Art to Science. In: Carley A.F., Davies P.R., Hutchings G.J., Spencer M.S. (eds) Surface Chemistry and Catalysis. Fundamental and Applied Catalysis. Springer, Boston, MA
(10) Khair, M. K.; Majewski, W. A. Diesel emissions and their control; SAE International, Warrendale, 2006.

(11) T. Seiyama, T. Arakawa, T. Matsuda, N. Yamazoe, and Y. Takita, Chem. Lett., 781 (1975)
(12) J.H. Kwak, D. Tran, J. Szanyi, C.H.F. Peden, J.H. Lee, Catal. Lett., 142 (2012), p. 295.
(13) ST Korhonen, DW Fickel, RF Lobo, BM Weckhuysen, AM Beale, Chemical Communications 47 (2), 800-802
(14) Negri, C.; Selleri, T.; Borfecchia, E.; Martini, A.; Lomachenko, K. A.; Janssens, T. V.W.; Cutini, M.; Bordiga, S.; Berlier, G. J. Am. Chem. Soc. 2020, 142, 15884−15896.

(15) J. H. Kwak, T. Varga, C. H. F. Peden, F. Gao, J. C. Hanson and J. Szanyi, J. Catal., 2014, 314, 83–93.
(16) Gao, F.; Mei, D. H.; Wang, Y. L.; Szanyi, J.; Peden, C. H. F. J. Am. Chem. Soc. 2017, 139, 4935−4942.
(17) Gao, F.; Walter, E. D.; Kollar, M.; Wang, Y.; Szanyi, J.; Peden, C. H. F. J. Catal. 2014, 319, 1−14.
(18) K. Khivantsev, J.-H. Kwak, N. R. Jaegers, J. Szanyi, Chemrxiv, 2020 DOI: 10.26434/chemrxiv.13134770
(19) Chen, H.-Y.; Collier, J. E.; Liu, D.; Mantarosie, L.; Durán- Martín, D.; Novák, V.; Rajaram, R. R.; Thompsett, D. Catal. Lett. 2016, 146 (9), 1706–1711.
(20) Khivantsev, K.; Jaegers, N. R.; Kovarik, L.; Hanson, J. C.; Tao, F. (Feng); Tang, Y.; Zhang, X.; Koleva, I. Z.; Aleksandrov, H. A.; Vayssilov, G. N.; Wang, Y.; Gao, F.; Szanyi, J. Angew. Chem. 2018, 130 (51), 16914–16919.
(21) Khivantsev, K.; Jaegers, N. R.; Kovarik, L.; Prodinger, S.; Derewinski, M. A.; Wang, Y.; Gao, F.; Szanyi, J. Appl. Catal. A. Gen. 2019, 569, 141–148.
(22) Khivantsev, K.; Jaegers, N. R.; Koleva, I. Z.; Aleksandrov, H. A.; Kovarik, L.; Engelhard, M.; Gao, F.; Wang, Y.; Vayssilov, G. N.; Szanyi, J. J. Phys. Chem. C 2020, 124 (1), 309–321.
(23) Khivantsev, K.; Gao, F.; Kovarik, L.; Wang, Y.; Szanyi, J. J. Phys. Chem. C 2018, 122 (20), 10820–10827.
(24) Moliner, M.; Corma, A. React. Chem. Eng. 2019, 4 (2), 223–234.
(25) Khivantsev, K.; Jaegers, N. R.; Kovarik, L.; Hu, J. Z.; Gao, F.; Wang, Y.; Szanyi, J. Emiss. Control Sci. Technol. 2019. DOI: 10.1007/s40825-019-00139-w

(26) E. Bello, V. J. Margarit, E. M. Gallego, F. Schuetze, C. Hengst , A. Corma, M. Moliner, Microporous and Mesoporous Materials 302 (2020) 110222.
(27) K. Khivantsev, N.R. Jaegers, L. Kovarik, M. Wang, J.Z. Hu, Y. Wang, M.A. Derewinski, J. Szanyi, Appl. Catal. B. 2021, 280, 119449
(28) K Khivantsev, J Szanyi, NR Jaegers, L Kovarik, F Gao, Y Wang, US Patent App. 16/546,641
(29) Ryou, Y. S.; Lee, J.; Cho, S. J.; Lee, H.; Kim, C. H.; Kim, D. Appl. Catal. B Environ. 2017, 212, 140–149.
(30) Ryou, Y. S.; Lee, J.; Lee, H.; Kim, C. H.; Kim, D. H., Catal. Today 2019, 320, 175–180.
(31) Lee, J.; Ryou, Y.; Hwang, S.; Kim, Y.; Cho, S. J.; Lee, H.; Kim, C. H.; Kim, D. H., Catal. Sci. Technol. 2019, 9 (1), 163–173.
(32) Kim, Y.; Hwang, S.; Lee, J.; Ryou, Y. S.; Lee, H.; Kim, C. H.; Kim, D. H. Emiss. Control Sci. Technol. 2019, 5 (2), 172–182.
(33) K. Khivantsev, X. Wei, L. Kovarik, N. R. Jaegers, E. D. Waler, P. Tran, Y. Wang, J. Szanyi, Chemrxiv 2020 DOI: 10.26434/chemrxiv.12385577
(34) H Zhao, X Chen, A Bhat, Y Li, JW Schwank, Applied Catalysis B: Environmental 2021, 282, 119611,
(35) H Zhao, X Chen, A Bhat, Y Li, JW Schwank, Applied Catalysis B: Environmental, 2021, 286, 119874.
(36) Dedecek, J.; Sobalík, Z.; Wichterlova , B. Catal. Rev.: Sci. Eng. 2012, 54, 135–223.
(37) Pashkova, V.; Klein, P.; Dedecek, J.; Tokarova, V.; Wichterlova, B. Microporous Mesoporous Mater. 2015, 202, 138–146.
(38) Gabova, V.; Dedecek, J.; Cejka, J. Chem. Commun. 2003, 1196–1197.
(39) Dedecek, J.; Balgova, V.; Pashkova, V.; Klein, P.; Wichterlova, B., Chem. Mater. 2012, 24, 3231–3239.
(40) Burton, A. W.; Zones, S. I. Stud. Surf. Sci. Catal. 2007, 168, 137–179.
(41) Lobo, R. F.; Zones, S. I.; Davis, J. Inclus. Phenom. Mol. 1995, 21, 47–78.

(42) K. Khivantsev, et. al. ChemCatChem, 2019, 10, 736-742.
(43) K.Hadjiivanov, E.Ivanova, M.Daturi, J.Saussey, J.-C.Lavalley, Chem. Phys. Lett. 2003, 370, 712-718.
(44) A. Mihaylova, K. Hadjiivanov, M. Che, J. Phys. Chem. B 2006, 110, 39, 19530–19536.
(45) Hadjiivanov, K. I., Catal. Rev. Sci. Eng. 2000, 42, 71-144.
(46) Hadjiivanov, K.; Saussey, J.; Freysz, J. L.; Lavalley, J. C., Catal. Lett. 1998, 52, 103–108.
(47) B. Tsyntsarski, V. Avreyska, H. Kolev, Ts. Marinova, D. Klissurski, K. Hadjiivanov, J. Mol. Catal. A: Chem. 193 (2003) 139–149.
(48) J. H. Lunsford, P. J. Hutta, M. J. Lin, and K. A. Windhorst, Inorg. Chem. 1978, 17, 3, 606–610.
(49) K. A. Windhorst, J. H. Lunsford, J. Am. Chem. Soc. 1975, 97, 6, 1407–1412.
(50) K. Chakarova, K. Hadjiivanov, Microporous and Mesoporous Materials 123 (2009) 123–128.

Competing interests: Authors have no conflicts to declare.

Acknowledgements

We would like to thank the financial support by Crosscut Lean Exhaust Emissions Reduction Simulations (CLEERS), which is an initiative funded by the U.S. Department of Energy (DOE) Vehicle Technologies Office to support the development of accurate tools for use in the design, calibration, and control of next generation engine/emissions control systems that maximize efficiency while complying with emissions regulations. M.A.D. was supported by the Materials Synthesis and Simulation Across Scales (MS3) Initiative conducted under the Laboratory Directed Research & Development Program at PNNL. Most experiments were conducted in the Environmental Molecular Sciences Laboratory (EMSL), a national scientific user facility sponsored by the Department of Energy's Office of Biological and Environmental Research at Pacific Northwest National Laboratory (PNNL). PNNL is a multi-program national laboratory operated for the DOE by Battelle Memorial Institute under Contract DE-AC06- 76RL01830.

Supplementary Information

Controlling Al-pair abundance in SSZ-13 zeolite via alkaline-earth metal assisted synthesis produces hydrothermally stable and active Co and Pd-SSZ-13 materials for pollutant abatement applications

Konstantin Khivantsev[1*]†, Miroslaw A. Derewinski[1,2*]†, Nicholas R. Jaegers[1], Daria Boglaienko[1], Xavier Isidro Pereira Hernandez[1], Carolyn Pearce[1], Yong Wang[1,3] and Janos Szanyi[1*]†

[1]Pacific Northwest National Laboratory Richland, WA 99352 USA

[2] J. Haber Institute of Catalysis and Surface Chemistry, Polish Academy of Sciences, Krakow 30-239, Poland

[3] The Gene and Linda Voiland School of Chemical Engineering and Bioengineering, Washington State University Pullman, WA 99164-6515

*corresponding authors: MAD, KK, JSz

†these authors contributed equally: KK , MAD, JSz

Na/SSZ-13 zeolite with Si/Al~10 was hydrothermally synthesized using the following recipe: 0.8 g of NaOH (Sigma Aldrich) was dissolved in 50 ml of deionized water. Then, 17 g of TMAda-OH (Sachem Inc., 25% N,N,N-trimethyl-1-adamantyl ammonium hydroxide) was added as a structure directing agent. Consequently, 0.75 g of $Al(OH)_3$ (Sigma Aldrich, ~54% Al_2O_3) was slowly added to the solution and stirred at 400 rpm until it was completely dissolved. Afterwards, 20.0 g of LUDOX HS-30 colloidal silica (Sigma Aldrich, 30 wt% suspension in H_2O) was added slowly to the solution until gel was formed.

The obtained gel was sealed in a 125 mL Teflon-lined stainless steel autoclave containing a magnetic stir bar. Hydrothermal synthesis was carried out at 160 °C under continuous gel stirring at 400 rpm for 4 days. After synthesis, the zeolite cake was separated from the suspension by centrifugation and washed three times with deionized water. It was then dried at 80 °C under N_2 flow overnight and calcined in air at 550 °C for 5 h in order to remove the SDA. NH_4/SSZ-13 was obtained by ion exchange of the as-prepared Na/SSZ-13 zeolite with 1 M ammonium nitrate solution solution at 80 °C for 5 h. The process was repeated two times.

Hydrothermal synthesis of Sr/SSZ-13 with Si/Al ~ 10 in the presence of $Sr(OH)_2$ was performed using similar recipe as for the Na/SSZ-13. However, in this case mole-equivalent amount of strontium hydroxide octahydrate (Sigma Aldrich) was used instead of NaOH. After synthesis, the zeolite cake was separated from the suspension by centrifugation and washed multiple times with deionized water. It was then dried at 80 °C under N_2 flow overnight and calcined in air at 550 °C for 5 h in order to remove the SDA.

NH_4/SSZ-13 was obtained by ion exchange of the as-prepared Sr/SSZ-13 zeolite with 1 M ammonium nitrate solution solution at 80 °C for 5 h. The process was repeated five times.

Cobalt(II) ion-exchange was performed by dispersing 1 g of NH_4-SSZ-13(Na) and NH_4-SSZ-13(Sr) powders in excess (150 ml) 2 M cobalt(II) nitrate (Sigma-aldrich) solution at 80 ºC with continuous stirring for 8 hours. Then, the powder was separated by centrifugation and washed with excess DI water 3 times (with centrifugation after each wash), dried at 80 ºC in air flow and subsequently calcined at 650 ºC for 4 hours.

Palladium tetramine nitrate (10% solution in water, Sigma-aldrich) was used to load 1.7 wt% Pd in Co-SSZ-13. More specifically, desired amount of palladium precursor solution was mixed with minimum amount of water (the total volume approximately equivalent to the pore volume of zeolite ~0.25 ml/g), then added drop-wise with a micropipette to Co-SSZ-13 powder.

Standard NOx adsorption tests were conducted in a plug-flow reactor system with powder samples (120 mg, 60–80 mesh) loaded in a quartz tube, using a synthetic gas mixture that contained ~200-220 or 27 ppm of NO, 250 ppm or 0 CO, 300 ppm or 3% H_2O, 14% or 20% O_2) balanced with N_2 at a flow rate of 300 sscm.

All the gas lines were heated to over 100 °C. Concentrations of reactants and products were measured by an online MKS MultiGas 2030 FTIR gas analyzer with a gas cell maintained at 191 °C. Two four-way valves were used for gas switching between the reactor and the bypass. Prior to storage testing at 100 °C, the sample was pretreated in air flow for 1 h at 550 °C and cooled to the target temperature in the same feed. The gas mixture was then switched from the reactor to the bypass, and desired concentration of NOx was added to the mixture. Upon stabilization, the gas mixture was switched back from bypass to the reactor for storage testing for 10 min. The sample was then heated to 650 °C at a rate of 10 °C/min to record the desorption profiles of gases in the effluent. Ambient-temperature measurements were performed with 120 mg of sample at 23 ºC by flowing ~27 ppm NO (with 20% oxygen, 300 ppm water balanced in nitrogen) at 300 sscm/min rate at constant temperature.

XANES experiments on Co/SSZ-13 samples were performed on bench-top easyXAFS instrument. Details about the instrument can be found elsewhere (reference: Seidler, G T; Mortensen, D R; Remesnik, A J; Pacold, J I; Ball, N A; Barry, N; Styczinski, M; Hoidn, O R. Review of scientific instruments online. , 2014, Vol.85(11), p.113906 ISSN: 0034-6748 , 1089-7623; DOI: 10.1063/1.4901599; PMID: 25430123). Approximately 150 mg of Co-SSZ-13 was pressed into a circular tablet with a press to give

tablet with sufficient thickness to provide enough E-jump during measurements. The Co-SSZ-13(Sr) saple had higher amount of Co which allowed us to collect high-quality XANES data with edge step of 0.54. Energy edge was calibrated using Co foil standard (comparing Co foil lab data with Co foil synchrotron data and accounting for the slight shift in energy).

The *in situ* static transmission IR experiments were conducted in a home-built cell housed in the sample compartment of a Bruker Vertex 80 spectrometer, equipped with an MCT detector and operated at 4 cm^{-1} resolution. The powder sample was pressed onto a tungsten mesh which, in turn, was mounted onto a copper heating assembly attached to a ceramic feedthrough. The sample could be resistively heated, and the sample temperature was monitored by a thermocouple spot welded onto the top center of the W grid. NO was cleaned with multiple freeze–pump–thaw cycles. Prior to spectrum collection, a background with the activated (annealed at 300 ºC) sample in the IR beam was collected. Each spectrum reported is obtained by averaging 256 scans.

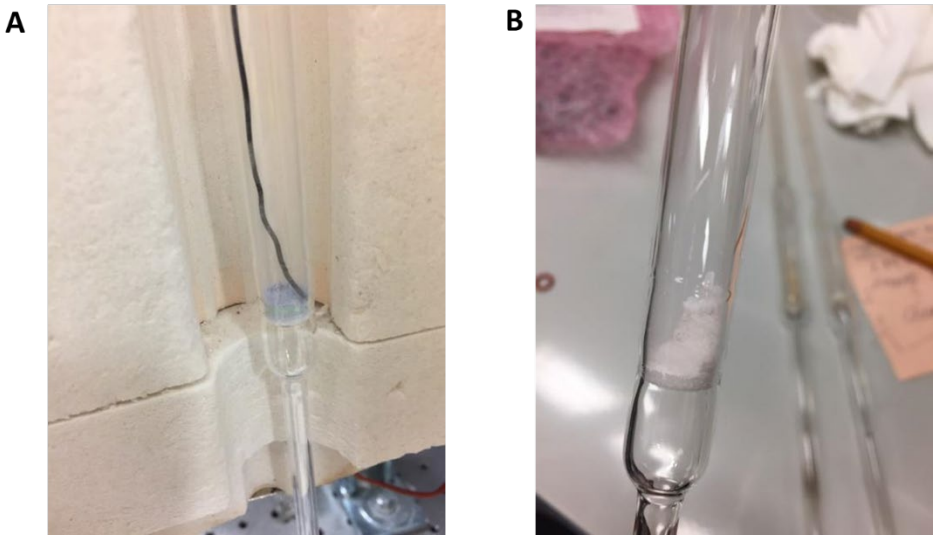

Fig. S1. A. Dehydrated Co-SSZ-13(Na) sample. Blue colour is due to presence of Co(II) cations in distorted tetrahedral ligand environment. B. The same sample exposed to ambient air for ~7 Days. This sample slowly adsorbs moisture from ambient air forming pink-ish Co(II)/SSZ-13 with hydrated octahedral (or square-pyramidal) Co(II) cations.

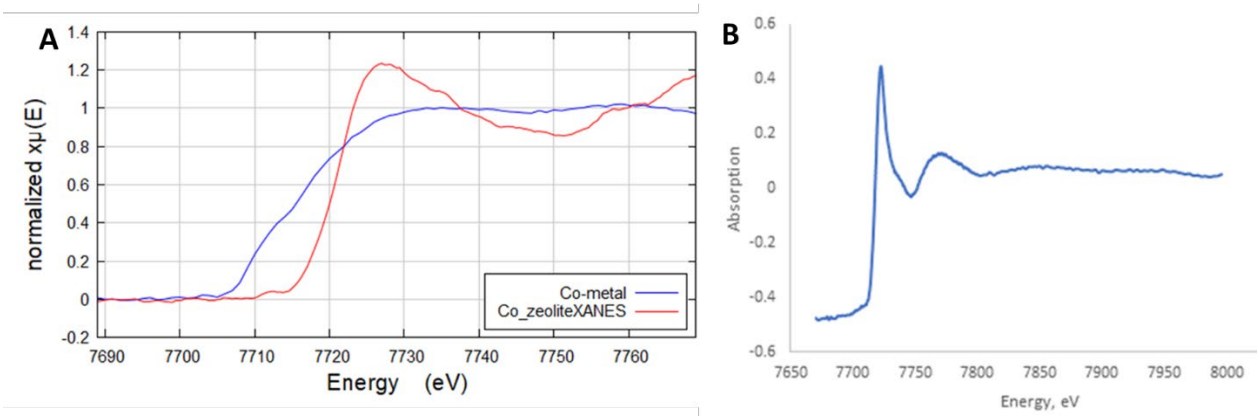

Fig. S2. A. Co K-edge XANES spectrum for Co-SSZ-13(Na) sample. Comparison with Co-metal foil is provided. B. Co K-edge XANES spectrum for Co-SSR-13(Sr).